LETTER • OPEN ACCESS

Arctic greening associated with lengthening growing seasons in Northern Alaska

View the article online for updates and enhancements.

Environmental Research Letters

LETTER

Arctic greening associated with lengthening growing seasons in Northern Alaska

Kyle A Arndt[1,2], Maria J Santos[3], Susan Ustin[2], Scott J Davidson[4], Doug Stow[5], Walter C Oechel[1,6], Thao T P Tran[7], Brian Graybill[1] and Donatella Zona[1,8]

1   Biology Department, San Diego State University, San Diego, CA, United States of America
2   Department of Land, Air and Water Resources, University of California at Davis, Davis, CA, United States of America
3   Department of Geography, University of Zurich, Zurich, Switzerland
4   Department of Geography and Environmental Management, University of Waterloo, Waterloo, ON, Canada
5   Department of Geography, San Diego State University, San Diego, CA, United States of America
6   Department of Geography, College of Life and Environmental Sciences, University of Exeter, Exeter, United Kingdom
7   Department of Earth and Planetary Science, University of California Berkeley, Berkeley, CA, United States of America
8   Department of Animal and Plant Sciences, University of Sheffield, Sheffield, United Kingdom

E-mail: karndt-w@sdsu.edu

Abstract

Many studies have reported that the Arctic is greening; however, we lack an understanding of the detailed patterns and processes that are leading to this observed greening. The normalized difference vegetation index (NDVI) is used to quantify greening, which has had largely positive trends over the last few decades using low spatial resolution satellite imagery such as AVHRR or MODIS over the pan-Arctic region. However, substantial fine scale spatial heterogeneity in the Arctic makes this large-scale investigation hard to interpret in terms of vegetation and other environmental changes. Here we focus on one area of the northern Alaskan Arctic using high spatial resolution (4 m) multispectral satellite imagery from DigitalGlobe™ to analyze the greening trend near Utqiaġvik (formerly known as Barrow) over 14 years from 2002 to 2016. We found that tundra vegetation has been greening ($\tau = 0.65$, $p = 0.01$, NDVI increase of $0.01\,\mathrm{yr}^{-1}$) despite no overall change in vegetation community composition. The greening is most closely correlated to the number of thawing degree days ($R^2 = 0.77$, $F = 21.5$, $p < 0.001$) which increased in a similar linear trend over the 14 year study period (1.79 ± 0.50 days per year, $p < 0.01$, $\tau = -0.56$). This suggests that in this Arctic ecosystem, greening is occurring due to a lengthening growing season that appears to stimulate plant productivity without any significant change in vegetation communities. We found that vegetation communities in wetter locations greened about twice as fast as those found in drier conditions supporting the hypothesis that these communities respond more strongly to warming. We suggest that in Arctic environments, vegetation productivity may continue to rise, particularly in wet areas.

1. Introduction

Vegetation trends are important to the carbon balance of Arctic ecosystems (Joos *et al* 2001, Mishra and Riley 2012). Organic carbon content in Arctic soils is about 1300 Pg (Hugelius *et al* 2014); roughly twice the current total atmospheric carbon content (IPCC 2013). Accelerated warming is occurring in the Arctic as a result of climate change and positive feedbacks (Chapin *et al* 2005, Serreze and Francis 2006, IPCC 2013) putting this large carbon pool at risk of loss to the atmosphere (Schuur *et al* 2013, Schuur *et al* 2015). Increasing permafrost temperatures (Romanovsky *et al* 2017), lateral flow of organic matter (Spencer *et al* 2015), and disturbance (Price *et al* 2013) are contributing to carbon losses. Carbon exchanges vary between wet and dry vegetation communities where wet communities (often standing water

dominated by wetland sedges) are typically characterized by strong uptake of carbon dioxide (CO_2) (Sturtevant and Oechel 2013, Treat *et al* 2018) and strong methane (CH_4) emissions (Davidson *et al* 2016b, Treat *et al* 2018). Dry communities (dominated by mosses, lichens and shrubs with a sub-surface water table) typically exhibit weaker uptake or sometimes net release of CO_2 and low emissions of CH_4 (Natali *et al* 2015, Treat *et al* 2018).

Changes in vegetation productivity have been measured by monitoring the normalized difference vegetation index (NDVI) calculated from satellite imagery (Jia *et al* 2003, Goetz *et al* 2005, Bhatt *et al* 2010). NDVI is positively correlated to vegetation biomass across Arctic tundra biomes (Jia *et al* 2003, Raynolds *et al* 2011, Epstein *et al* 2012) therefore NDVI increases are defined as 'greening' and NDVI decreases are defined as 'browning'. Researchers have detected greening trends across the pan-Arctic over the past several decades (Jia *et al* 2003, Bhatt *et al* 2010, Bhatt *et al* 2014); however, greening trends have started to weaken (Piao *et al* 2014) or reverse with large browning areas, specifically in the European Arctic and Seward Peninsula (Bhatt *et al* 2013, Phoenix and Bjerke 2016, Bhatt *et al* 2017, Lara *et al* 2018).

Greening has predominantly been attributed to large-scale climate conditions including rising temperatures linked to reduced albedo over the ocean due to sea ice decline (Bhatt *et al* 2010, Bhatt *et al* 2014, Macias-Fauria *et al* 2017). In lower latitude Arctic regions, greening has been associated with shrub encroachment (Tape *et al* 2006, Forbes *et al* 2010, Myers-Smith *et al* 2011), which also has a positive feedback with warming (Chapin *et al* 2005). Greening has also been correlated to shifting moisture regimes (Bhatt *et al* 2017, Westergaard-Nielsen *et al* 2017) and increases in temperature and precipitation due to movements of air masses from lower latitudes (Macias-Fauria *et al* 2017).

Most studies on Arctic greening use coarse satellite imagery including AVHRR and MODIS with spatial resolutions of 1–8 km and 0.25–1 km, respectively. These images provide broad coverage of the pan-Arctic, are relatively continuous temporally, and are useful for determining global trends. However, due to the coarse spatial resolution, fine details of patterns and processes are indiscernible and has limited our understanding of greening and browning (Bartsch *et al* 2016, Myers-Smith *et al* 2019), particularly in ecosystems characterized by fine spatial heterogeneity such as Arctic tundra (Webber 1978, Billings and Peterson 1980).

Recent studies have taken more detailed approaches to assess greening in the Arctic by utilizing Landsat satellites (30 m spatial resolution) (Frost *et al* 2014, Nitze and Grosse 2016, Raynolds and Walker 2016, Lara *et al* 2018). Some studies found that browning can be muddled by surface water due to the strong absorption radiance by water despite greening of vegetation (Raynolds and Walker 2016). Others have shown how

the heterogeneity of vegetation cover, geomorphic landscape type, and climate regimes can impact the rate and trend of greening (Lara *et al* 2018). While Landsat's 30 m spatial resolution is able to cover a large spatio-temporal extent, it does not fully capture the heterogeneity within Arctic ecosystems, which have fine scale polygonal landforms often less than 30 m across (Webber 1978, Billings and Peterson 1980).

Here we present a high spatial resolution (4 m) analysis of greening for an area near Utqiaġvik (formerly Barrow), Alaska. As more high spatial resolution satellite imagery is collected, these time-series approaches will become increasingly valuable (Stow *et al* 2004) and offer new opportunities and challenges for studying these complex, heterogeneous ecosystems. These tools and their results will likely prove beneficial for modeling carbon dynamics over multiple scales and validating trends reported by larger scales studies. In our study, we aim to (1) show if vegetation communities have changed, (2) analyze fine-scale spatial NDVI trends, and (3) assess correlates of shifts in vegetation communities and NDVI.

2. Methodology

2.1. Study Area

Our study was conducted on the Barrow Environmental Observatory (BEO) located near Utqiaġvik, Alaska (figure 1). The BEO has a long research history, resulting in a high frequency of satellite tasking, a relatively steady meteorological data record, and accessible field sites. Located in the Arctic Coastal Plain, the site is on continuous permafrost and consists of several drained lake basins (hereby basins), differing in time since drainage (Hinkel *et al* 2003), and ice-wedge polygon formations due to a seasonal freeze-thaw cycle (Webber 1978). Dominant vegetation in the region is characterized as a sedge/grass moss wetland (Walker *et al* 2005). Further details are available in the supplementary material is available online at stacks.iop.org/ERL/14/125018/mmedia.

2.2. Imagery data acquisition and pre-processing

Imagery used in this study was procured through the Polar Geospatial Center at the University of Minnesota (table 1). Acquisition dates spanned 14 years, with the earliest Ikonos image acquired 18 July 2002 and the final WorldView-3 image acquired 24 July 2016. A digital elevation model (figure 1(b)) was used to measure the relative elevation of features (Wilson *et al* 2013). The largest overlapping area in all images defined the study area extent with the northwest corner at 71 °19′34.36″ N, 156 °41′20.62″ W and the southeast corner at 71 °16′9.02″ N, 156 °31′26.44″ W. The total study area was 37.42 km². Supplementary materials provide details on image pre-processing.

Figure 1. (a) An overview of the study area showing the location of Utqiaġvik in Alaska represented by a red star. The study area extent is highlighted with a red box in the true color RGB mosaic acquired 22 July 2015 by WV2. (b) Basins over the study area; colors represent the age of basins according to Hinkel *et al* (2003). The blue is the only young age basin in the study area (basin 1). There were eight medium age basins (purple) and eight old basins (yellow). Basin numbers are labelled according to age and then generally north to south. (c) Digital elevation model coverage through the study area. There is a gentle slope from the southern extent to the north with tributaries to the Elson Lagoon and basins as the lowest parts across the landscape. The background of panels b and c are a true-color RGB image taken 24 July 2016 by WV3.

2.2.1. Meteorological data

Hourly air temperature and relative humidity data from the Barrow Atmospheric Baseline Observatory (BRW, NOAA), located north of the study area (71.3230 $^{\circ}$N, 156.6114 $^{\circ}$W), were used to understand climatic conditions during growing seasons. Mean growing season (June–August) air temperature, vapor pressure deficit (VPD), growing degree days (GDD, cumulative mean daily air temperature over 0 $^{\circ}$C), and thawing degree days (TDD, cumulative number of days with a mean air temperature over 0 $^{\circ}$C) were calculated. TDD and GDD were calculated for image acquisition dates allowing NDVI comparisons.

2.3. Field data collection

Field surveys were conducted in July 2018. Eight transects were surveyed with a total of 2971 m × 1 m plots. Transects ranged from 100 to 300 meters in

length and plots were surveyed every 5 m. For each plot, plant types (grass, moss, lichen, shrub, open water, and forb), thaw depth, soil moisture, and canopy height were measured (see supplementary materials for descriptions of field techniques). Medians and standard deviations are reported as summary statistics. Coordinates of plots were recorded using a Trimble 5700 differential global positioning system (Trimble$^{\circledR}$, USA).

2.4. Random forest vegetation model

Pixels with NDVI value below 0.1 (Gandhi *et al* 2015) were masked to remove snow and water, which have extremely high or low reflectance. Then we used histogram matching to color correct images with the 2016 WorldView-3 image as the base (results in supplementary material). Bright and dark objects were removed by the NDVI filter, therefore these objects

Table 1. Inventory of the images used for the study including the acquisition date of the image and the sensor used. All imagery used were DigitalGlobe™ assets (© Maxar Technologies, USA). Sensors are as follows: IKO, Ikonos; QB2, QuickBird-2; WV2, WorldView-2; WV3, WorldView-3. July and August images were used in time-series analysis.

Acquisition date	Sensor
18-July-02	IKO
02-August-02	QB2
16-June-06	QB2
21-July-10	WV2
24-July-10	WV2
25-July-10	WV2
03-August-10	WV2
10-July-11	WV2
05-July-12	WV2
13-August-12	WV2
30-June-14	WV2
24-June-15	WV2
22-July-15	WV2
20-July-16	WV2
24-July-16	WV3

will not skew histograms and allow for a better comparison of illumination. A tasseled cap transformation was done to produce three orthogonal polynomial combinations representing brightness, wetness, and greenness of objects (Kauth and Thomas 1976, Yarbrough *et al* 2005).

Vegetation community classes from 'wet' and 'dry' locations were chosen based on functional relationships with carbon cycling (Sturtevant and Oechel 2013, Natali *et al* 2015, Davidson *et al* 2016b, Treat *et al* 2018) and being spectrally separable. An additional open water class was included after vegetation classification; corresponding to pixels removed by the NDVI filter. We utilized a random forest machine learning algorithm for the vegetation classification model because of its high accuracy when predicting vegetation classes (Chapman *et al* 2009, van Beijma *et al* 2014). Four spectral bands (blue, green, red, and near-infrared (NIR)) and three tasseled cap variables were used to train the random forest model. Welch two sample t-tests were used to test for significant differences in spectral properties between vegetation communities (see supplementary material). The random forest model was then applied to all 15 images for predicting vegetation communities. Model accuracy was assessed using 30% of ground reference points not used in model training, against the classification of the latest 24 July 2016 WorldView-3 image.

2.5. Greening assessment
Greening of vegetation was measured using NDVI following many Arctic studies (Bhatt *et al* 2010, Epstein *et al* 2012, Bhatt *et al* 2013). Changes in NDVI

were estimated prior to applying the NDVI threshold and histogram matching, since open water can contribute to browning (Raynolds and Walker 2016) which, we wanted to capture. Since NDVI changes most rapidly during green-up (Zhang *et al* 2018), differs seasonally and saturates (Suzuki *et al* 2001), only peak season (mid-July to early August) image acquisitions were used in the time-series analysis. This approach captured NDVI shifts linked to long term changes instead of seasonal differences due to acquisition dates. We also calculated a pixel level change to locate finely detailed space-time anomalies by regressing each pixel's NDVI over time.
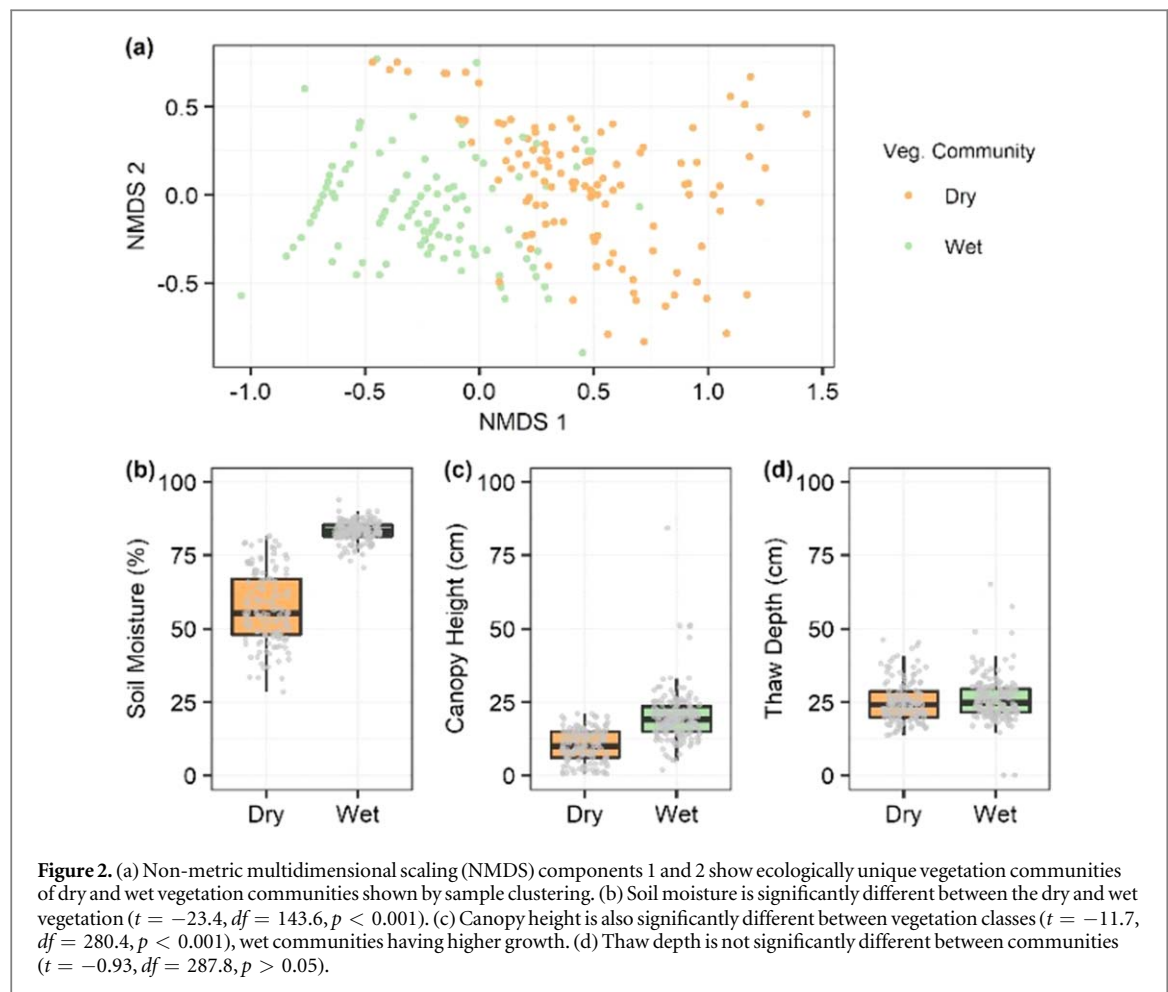
2.6. Statistical analyzes
Non-metric multidimensional scaling (NMDS) was used to determine ecological separability between vegetation communities using the 'vegan' package (Oksanen *et al* 2018). Differences in the physical environmental parameters were determined using Welch two sample t-tests; the t-statistic (t), degrees of freedom (df), and p-value (p) are reported for these tests. Homogeneity of variance was tested for all parameters before significance testing.

Changes in vegetation coverage, NDVI, and TDD over time were calculated according to Yue *et al* (2002) using the 'zyp' package (Bronaugh and Werner 2019), which is sensitive to potential autocorrelation in time-series data. These changes were analyzed over the entire image and by separating the landscape into the following age based categories of basins (Hinkel *et al* 2003): young basins (0–50 years old), medium basins (50–300 years old), old basins (300–2000 years old), and the 'other' category that accounts for the remaining landscape (figure 1(a)). Before analyzing controls on NDVI, data were detrended to avoid temporal autocorrelation by taking the residuals of the least squares linear model between year and the given variable.

NDVI controls were analyzed using linear mixed effects models (LMEs) using maximum likelihood in the 'nlme' package (Pinheiro *et al* 2018) and the 'MuMIn' package (Barton 2019) was used to calculate the coefficient of determination of these LMEs. Two components of coefficients of determination are reported for each LME, marginal (R_m^2) and conditional (R_c^2), representing the coefficient of fixed effects and full model respectively. LMEs were compared to a null model with only year as a temporal random effect using analysis of variance. LMEs included single variable models with each variable as fixed variables (GDD, TDD, mean air temperature, and mean VPD) and a full multivariate model with TDD, mean air temperature, and mean VPD.

To determine pixel level greening and browning trends, the Theil–Sen slope method (Sen 1968, Theil 1992) was used for the rate of change and

Figure 2. (a) Non-metric multidimensional scaling (NMDS) components 1 and 2 show ecologically unique vegetation communities of dry and wet vegetation communities shown by sample clustering. (b) Soil moisture is significantly different between the dry and wet vegetation ($t = -23.4$, $df = 143.6$, $p < 0.001$). (c) Canopy height is also significantly different between vegetation classes ($t = -11.7$, $df = 280.4$, $p < 0.001$), wet communities having higher growth. (d) Thaw depth is not significantly different between communities ($t = -0.93$, $df = 287.8$, $p > 0.05$).

Yue *et al* (2002) time-series methods were again used to determine statistical significance. This method of trend detection performs better in remote sensing data than more basic least-squares regression (Fernandes and Leblanc 2005). NDVI of each pixel over time was regressed using the 'spatialEco' package (Evans 2019), resulting in rasters of Kendall's τ statistics (ranging from −1 to 1 with values closer to 0 indicating no significant trend) and Theil–Sen slope. All statistical analyzes were conducted using R v.3.5.2 statistical software (R Core Team 2018).

3. Results
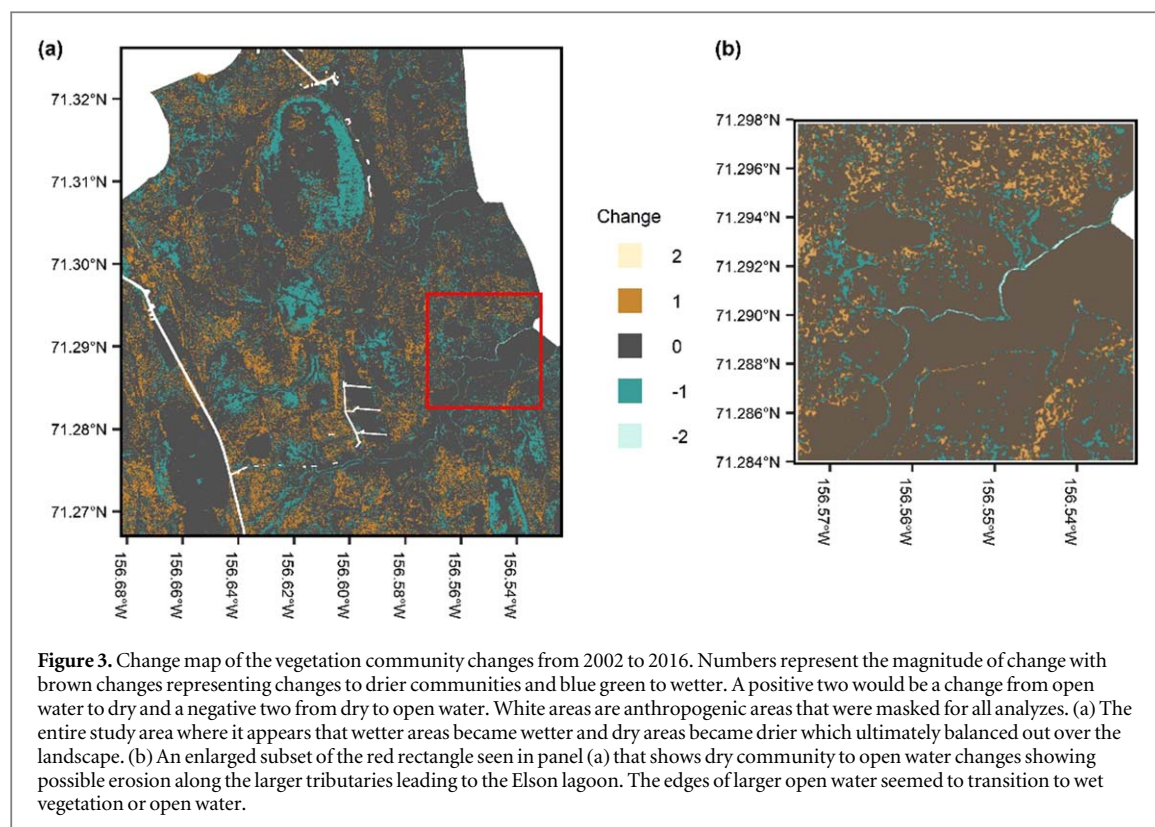
3.1. Vegetation community differentiation
Vegetation communities were separable with NMDS showing distinct communities based on vegetation composition (figure 2(a)), and environmental conditions (figures 2(b)–(d)). Soil moisture was 55.09% ± 12.40% and 83.18% ± 3.33% for dry and wet communities respectively, and significantly different ($t = -23.4$, $df = 143.6$, $p < 0.001$, figure 2(b)). Canopy heights were also significantly different ($t = -11.7$, $df = 280.4$, $p < 0.001$, figure 2(c)), with higher wet than dry vegetation (19 ± 8.99 cm and 10 ± 5.49 cm, respectively). Thaw depths were not

significantly different between communities with depths of 24.0 ± 7.2 cm and 24.7 ± 7.9 cm for dry and wet communities ($t = -0.93$, $df = 287.8$, $p = 0.35$, figure 2(d)).

3.2. Vegetation classification
The random forest vegetation classification had 82% overall accuracy. Producer's accuracy was slightly higher for wet communities (86%) than dry communities (78%) and user's accuracy was comparable for wet (83%) and dry (82%) communities. Twenty-five bootstrapped repetitions of the training data for random forest model yielded an overall accuracy of 89%.

Change detection between imagery dates revealed negligible change in the overall areal extent of vegetation communities from 2002 to 2016. There was about a half percent loss of dry community area (16 ha) corresponding mostly to gains in open water (15 ha) and a small increase in the wet community (1 ha), in line with errors in areal estimates stemming from image classification. A 2002–2016 change map (figure 3) showed spatial trends of wetter areas becoming wetter and drier areas becoming drier which, appear relatively balanced from the total analysis.

Figure 3. Change map of the vegetation community changes from 2002 to 2016. Numbers represent the magnitude of change with brown changes representing changes to drier communities and blue green to wetter. A positive two would be a change from open water to dry and a negative two from dry to open water. White areas are anthropogenic areas that were masked for all analyzes. (a) The entire study area where it appears that wetter areas became wetter and dry areas became drier which ultimately balanced out over the landscape. (b) An enlarged subset of the red rectangle seen in panel (a) that shows dry community to open water changes showing possible erosion along the larger tributaries leading to the Elson lagoon. The edges of larger open water seemed to transition to wet vegetation or open water.

3.2.1. Vegetation composition by basin age

There was no noticeable change in vegetation community composition in the young basin with overall changes less than 1% (< 1 ha). Medium age basins by contrast showed a 16% increase in wet communities (85 ha) corresponding to similar losses in dry communities. Old basins had a 4% decrease in wet communities (26 ha) and similar increase in dry communities (24 ha). The remainder of the landscape showed little change with wet communities decreasing by 3% and dry communities increasing by the same amount. The only significant trend was open water in the 'other' landscape area ($\tau = 0.77$, $p = 0.002$, slope $= 0.72$ ha/year). All other trends were not significant.

3.2.2. Vegetation change at individual basins

Some significant trends in vegetation cover were observed within specific basins (table 2). Three medium age basins (3, 4 and 5) had significant increases in wet communities which, corresponded to losses in dry communities. Conversely, old basin number 10 gained dry community area but had no clear reciprocal change in open water or wet communities. Since there was only one young basin, these results do not differ from above finding no significant change.

3.3. Greening of the landscape

We found an overall greening trend over the entire study area ($\tau = 0.65$, $p = 0.01$, NDVI increase of 0.01 yr^{-1}) and within all basins, except for th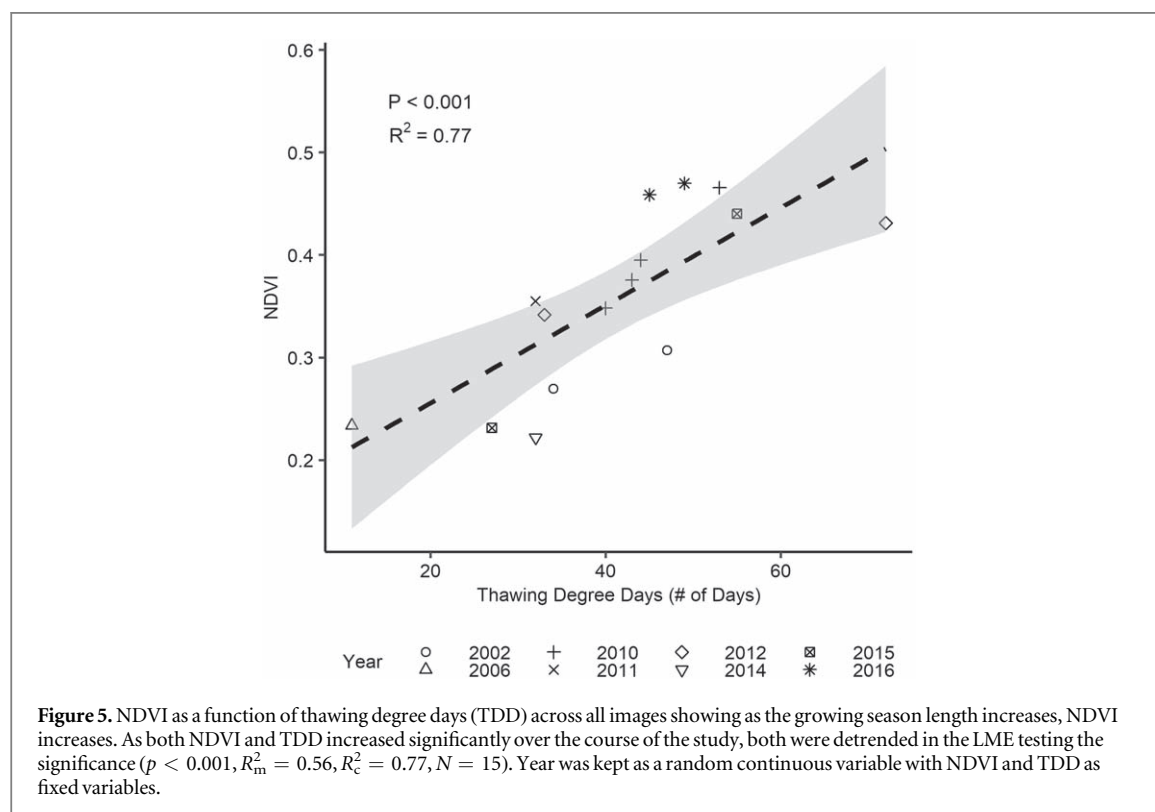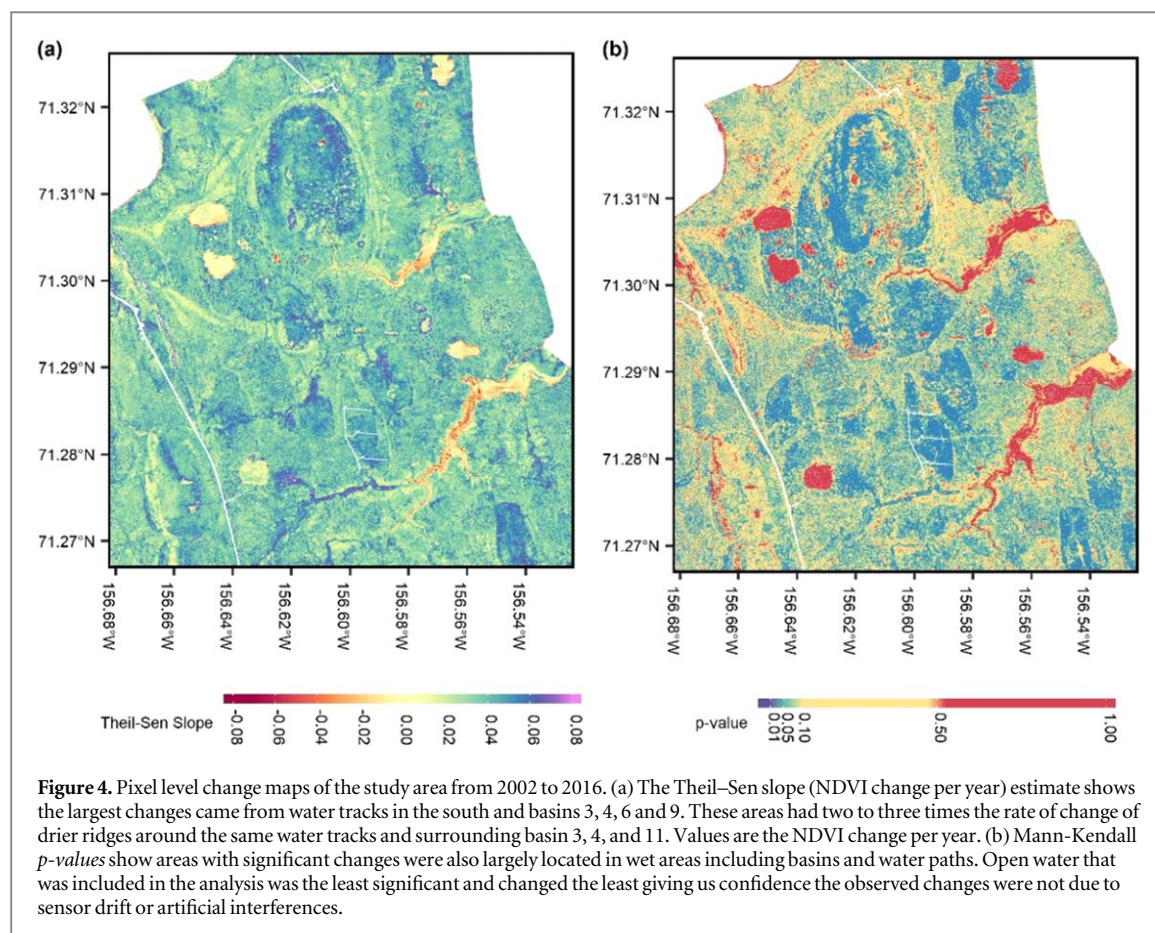e young basin, which showed a slight increase with no significant change ($p = 0.077$, $\tau = 0.45$, table 2). We also found that the NDVI trend with respect to basin age is spatially variable with faster rates of greening in medium basins than old or 'other'. Both wet and dry vegetation communities significantly increased in NDVI as well ($\tau = 0.65$, $p = 0.01$ for both wet and dry communities). The rate of increase in NDVI was faster for wet communities (0.013 ± 0.003 yr^{-1}) than for dry communities (0.011 ± 0.002 yr^{-1}). Pixel level analysis showed similar results to those aggregated by basins or vegetation. Wet areas showed the largest change with rates of NDVI change around 0.05–0.08 y^{-1}. Dry ridges show NDVI changes closer to 0.01–0.04 y^{-1} (figure 4).

3.3.1. NDVI controls

TDD had the strongest correlation with NDVI (figure 5, $F = 21.5$, $p < 0.001$, $R_m^2 = 0.56$, $R_c^2 = 0.77$, NDVI increase of 0.004 ± 0.001 d^{-1}) and explained most of the variability (the full multivariate model was not significantly different from the individual model of TDD ($p = 0.88$, likelihood ratio $= 0.25$)). GDD also strongly correlated with NDVI, with a slightly lower correlation coefficient than TDD ($F = 20.7$, $p < 0.001$, $R_m^2 = 0.52$, $R_c^2 = 0.77$, NDVI increase of 0.0008 ± 0.0002 °C^{-1}). As GDD was strongly collinear with TDD, they were not assessed together in any model ($F = 74.7$, $p < 0.001$, $R^2 = 0.84$). Mean growing season air temperature and VPD were not correlated to NDVI ($F = 1.2$, $p = 0.27$ for air temperature and $F = 0.53$, $p = 0.45$ for VPD). The first day of the year with a mean air temperature above freezing

Table 2. Time-series statistics for each individual basin with regards to the NDVI and vegetation communities. Units for the vegetation communities are in hectares. The *p*-value is derived from Kendall's Tau and the slope is derived from Theil–Sen.

Basin number	Basin age	Dry			Wet			Water			NDVI		
		p-value	Tau	Slope	*p*-value	Tau	Slope	*p*-value	Tau	Slope	*p*-value	Tau	Slope
1	Young	0.421	0.216	0.223	0.334	−0.256	−0.216	1.000	0.198	−0.365	0.077	0.452	0.009
2	Medium	0.053	0.492	0.438	0.077	−0.452	−0.419	0.629	−0.138	0.050	0.016	0.610	0.013
3	Medium	0.036	−0.531	−2.931	0.036	0.531	2.846	0.006	0.688	0.039	0.024	0.570	0.013
4	Medium	0.016	−0.610	−1.125	0.016	0.610	1.125	1.000	0.000	−0.002	0.010	0.649	0.014
5	Medium	0.036	−0.531	−0.627	0.036	0.531	0.627	N/A	N/A	N/A	0.006	0.688	0.015
6	Medium	1.000	0.198	−0.049	1.000	1.000	0.079	1.000	0.010	−0.185	0.006	0.688	0.013
7	Medium	0.077	0.452	−0.142	0.077	−0.452	0.154	1.000	0.518	0.003	0.006	0.688	0.016
8	Medium	1.000	0.053	−0.368	0.053	0.492	0.031	N/A	N/A	N/A	0.006	0.688	0.015
9	Medium	0.147	−0.374	−0.697	0.147	0.374	0.697	N/A	N/A	N/A	0.006	0.688	0.016
10	Old	0.010	0.649	0.068	1.000	0.198	−0.540	1.000	0.260	−0.078	0.016	0.610	0.013
11	Old	0.872	0.059	0.235	0.872	0.059	−0.117	0.747	−0.098	0.134	0.010	0.649	0.011
12	Old	0.260	−0.295	−0.111	0.334	0.256	0.034	1.000	−0.020	0.012	0.010	0.649	0.012
13	Old	0.260	0.295	0.421	0.520	−0.177	−0.399	1.000	0.334	−0.291	0.016	0.610	0.011
14	Old	0.334	−0.256	−0.133	0.260	0.295	0.275	0.077	−0.452	−0.069	0.010	0.649	0.012
15	Old	1.000	1.000	12.125	0.872	0.059	−0.951	0.147	−0.374	−0.268	0.016	0.610	0.011
16	Old	0.107	−0.413	−0.643	1.000	0.107	7.255	1.000	0.421	−0.180	0.010	0.649	0.013
17	Old	0.629	−0.138	−0.133	0.629	0.138	0.131	1.000	0.162	−0.003	0.006	0.688	0.013
Other	N/A	1.000	0.872	31.090	1.000	0.020	−4.096	0.002	0.767	0.619	0.010	0.649	0.011

Figure 4. Pixel level change maps of the study area from 2002 to 2016. (a) The Theil–Sen slope (NDVI change per year) estimate shows the largest changes came from water tracks in the south and basins 3, 4, 6 and 9. These areas had two to three times the rate of change of drier ridges around the same water tracks and surrounding basin 3, 4, and 11. Values are the NDVI change per year. (b) Mann-Kendall *p-values* show areas with significant changes were also largely located in wet areas including basins and water paths. Open water that was included in the analysis was the least significant and changed the least giving us confidence the observed changes were not due to sensor drift or artificial interferences.

Figure 5. NDVI as a function of thawing degree days (TDD) across all images showing as the growing season length increases, NDVI increases. As both NDVI and TDD increased significantly over the course of the study, both were detrended in the LME testing the significance ($p < 0.001$, $R^2_m = 0.56$, $R^2_c = 0.77$, $N = 15$). Year was kept as a random continuous variable with NDVI and TDD as fixed variables.

(i.e. first TDD) significantly shifted towards an earlier date at a rate of 1.07 d per year ($\tau = -0.47$, $p = 0.02$) but we found no evidence for changes in the last day above freezing ($\tau = -0.01$, $p = 1$).

4. Discussion

4.1. Vegetation community characteristics
Vegetation community groupings based on functional differences in carbon cycling characteristics (Sturtevant and Oechel 2013, Davidson *et al* 2016b, Treat *et al* 2018), proved to be spectrally separable agreeing with prior studies (Lin *et al* 2012, Davidson *et al* 2016a). We were able to obtain ecological separation between vegetation communities as well using surveys of plant types (e.g. graminoid, moss, lichen, etc).

Soil moisture content was the main environmental factor driving the separation of the vegetation communities and dictating their geographical distribution. Our results agree with findings from past studies (Lin *et al* 2012) that showed vegetation communities near Utqiaġvik exist across a moisture gradient. Canopy heights differed between communities, with taller vegetation in wet communities and shorter vegetation in dry communities; canopy height has been used as a correlative metric for predicting above ground biomass in Arctic ecosystems (Berner *et al* 2018). This suggests that wet communities typically have higher biomass than dry communities and therefore the relationship between biomass and moisture may exist as well (see supplementary material). Thaw depth did not differ between communities but this does not necessarily imply equal carbon storage in the active layer beneath the vegetation due to usually higher concentrations of organic matter in wetter lowlands, i.e. higher biomass given equal soil volume (Ping *et al* 2008).

4.2. Vegetation community shifts at the landscape scale
We observed no shift in the overall cover of vegetation communities over the 14 year study. Measured shifts were around 1% and could be due to differences in water table, other seasonal differences, or classification errors. These results are in line with prior long-term studies of vegetation communities in this area showing 3% change over 60 years (1948–2008) when using high spatial resolution photography with satellite imagery (Lin *et al* 2012). However, Lin *et al* (2012) used four single images (1948, 1955, 1979 and 2008) to assess vegetation community change in their study which, did not account for intra-annual variability in standing water, a possible source of error. The seasonal progression in our data during 2010, where four images were acquired over two weeks (21 July–3 August), showed a seasonal drying. Changes in surface water during the season can erroneously translate into error in predicted cover of vegetation communities by the random forest model. This result highlights the importance of considering timing of acquisition of high spatial resolution imagery in analyzing interannual patterns and change over long timescales.

Vegetation changes were observed in more localized areas. The young basin vegetation communities did not change and consisted mostly of wet vegetation. Old basins, comprised largely of low center polygons, are thawing where ice wedge degradation occurs over time scales ∼60 years; the stage of degradation determines the degree to which the landscape is wet or dry (Liljedahl *et al* 2016). We saw no overall significant changes in vegetation communities through the time-series but that does not mean degradation and shifts are not occurring. Polygon degradation effects could balance out if multiple stages are occurring simultaneously over the entire study area. According to our results, most changes occurred in medium and old age basins where medium age basins gained wet and lost dry communities and old age basins showed the opposite process (table 2, figure 3). Polygon degradation (Liljedahl *et al* 2016) in old basins could increase drainage to the lowest part of the nearby landscape, medium basins, due to interconnected troughs and could explain increases in wetness in these medium basins. This is supported by the change map showing the wetting in these medium basins and drying along the edges (figure 3(a)). This is also supported by the fact that medium basins had the lowest elevations (figure 1(b)). Evidence of erosion or rising water levels exists where edges of water paths have gains in wet communities and edges of larger tributaries show dry vegetation to open water transitions (figure 3(b)). These results suggest that even though total vegetation community compositions have not changed over the entire study area, high spatial resolution imagery allows us to detect localized but relatively balanced shifts.

4.3. Greening of the landscape
4.3.1. Landscape scale greening trends
We found evidence of greening across vegetation communities and basins. Mean NDVI values of the whole image, split by vegetation type, basin age, and individual basins, displayed significant increasing trends in NDVI in all areas except the young basin. However, the young basin already had a relatively high NDVI (0.6 in 2016) and is at or above observed peaks for this ecosystem (Bhatt *et al* 2017, May *et al* 2017). Increases in NDVI can be due to changes in land cover type (Elmendorf *et al* 2012) or increased vegetation biomass (Hudson and Henry 2009). Due to the lack of change in total vegetation community composition, we suggest that the most likely explanation for the observed greening in this ecosystem is increased plant productivity and growth.

4.3.2. Vegetation community specific greening rates

Our results show vegetation communities greening at different rates, in agreement with prior studies (May *et al* 2017, Andresen *et al* 2018). This trend has been locally shown to stand across the North Slope of Alaska where wet communities green faster under warming (May *et al* 2017). Further, at a species level, wet communities have been observed to shift more than dry communities in this region over time, with sedge species replacing bryophytes (Villarreal *et al* 2012), which could aid in NDVI increases. When trends for each pixel were analyzed, spatial patterns became even more evident (figure 4). Some wet areas including many medium age basins (basins 2, 4, 6 and 9) and lower lying water paths had some of the highest rates of greening, sometimes more than double that of dry ridges (figure 4). The *p*-value map also supported that these same areas have more instances significant change. The faster green up in wet areas confirms studies that show increases in moisture, expected in this region under climate predictions (Zhang *et al* 2012), can enhance greening. Increases in moisture do not universally increase NDVI as shown in Raynolds and Walker (2016), where standing water depressed NDVI due to differential absorption of NIR and red irradiance by water. Lara *et al* (2018) further showed negative correlations between precipitation and NDVI.

4.3.3. NDVI controls and growing season length

Greening was most correlated to increases in TDD, agreeing with previous studies (Huemmrich *et al* 2010, Zeng *et al* 2011). This further suggests that NDVI is most influenced by the thawing date (Oberbauer *et al* 2013, Andresen *et al* 2018); however, this may not always be true. If there is a freezing day after initial thaw, an early thawing can have the opposite effect on growth (Oberbauer *et al* 2013), which causes browning (Phoenix and Bjerke 2016). Mean temperature and VPD did not influence NDVI in our study, possibly because temperature and VPD have been shown to correlate with max NDVI (Epstein *et al* 2012, Bhatt *et al* 2014, Bhatt *et al* 2017) which we were are unable to calculate with limited image acquisitions. Further, the temperature-NDVI relationship has been seen to weaken recently in the Arctic (Piao *et al* 2014).

Many larger scale and coarser resolution studies have used the summer warmth index (SWI), the sum of mean monthly temperatures (Jia *et al* 2003), to explain NDVI trends (Bhatt *et al* 2010, Bhatt *et al* 2013, Bhatt *et al* 2014, Bieniek *et al* 2015, Bhatt *et al* 2017, Berner *et al* 2018). SWI works for coarse-scale pan-Arctic studies that use maximum or time-integrated NDVI and have one value that represents the full growing season. However, in high spatial resolution investigations such as our study, a metric like TDD, that's measured on the acquisition date will better explain NDVI. Due to the tie between TDD and NDVI, we suggest that for high Arctic communities, if thawing continues to start earlier, then continued increases in NDVI are expected.

NDVI and vegetation communities differed seasonally in 2010 when four images were acquired within two weeks. This emphasizes that temporal and spatial events may greatly affect NDVI values observed. We accounted for this by only using images acquired closer to peak growing season. While intraannual variability was observed in NDVI, the relationship with TDD, which also increased over the study period, gives us confidence in the overall greening trend. Further, these multiple images were used in time series analyzes including the variability in trend analysis. Ultimately more satellite tasking and image acquisitions would be ideal to continue monitoring this trend. More meteorological data, such as precipitation and evapotranspiration would be ideal to tease out larger scale influences on NDVI (Andresen and Lougheed 2015). Unfortunately, these datasets are not always available over longer time-series or spatial domains, especially within remote areas like the Arctic.

5. Conclusion

We found evidence of greening across the landscape, particularly in wet areas, and a balanced shift in vegetation communities. TDD was best correlated to the positive greening signal. There was no large shift in vegetation community assemblage, but localized changes were observed showing spatially variable wetting and drying. Our study emphasizes the increased ability of high-resolution remote sensing to analyze details in change detection analyzes in the Arctic. Specifically, we were able to observe that wet communities may respond to warming at a faster rate than drier communities.

Our study analyzes a small area in the Arctic but takes a detailed approach to understanding Arctic greening. Many studies have looked at large scale changes which are important in a global context but lack detailed explanations (Myers-Smith *et al* 2019). Only by understanding drivers of greening can we more accurately predict future vegetation productivity in the Arctic, which is currently of great importance given that experts cannot currently agree on the direction of change of the carbon balance (Abbott *et al* 2016).

Data availability statement

The data that support the findings of this study are openly available at https://doi.org/10.25412/iop.10324745.v1.

ORCID iDs

Kyle A Arndt ⓘ https://orcid.org/0000-0003-4158-2054

Maria J Santos ⓘ https://orcid.org/0000-0002-6558-7477

Susan Ustin ⓘ https://orcid.org/0000-0001-8551-0461

Scott J Davidson ⓘ https://orcid.org/0000-0001-8327-2121

Doug Stow ⓘ https://orcid.org/0000-0001-5246-7073

Walter C Oechel ⓘ https://orcid.org/0000-0002-3504-026X

Donatella Zona ⓘ https://orcid.org/0000-0002-0003-4839

References

Abbott B W *et al* 2016 Biomass offsets little or none of permafrost carbon release from soils, streams, and wildfire: an expert assessment *Environ. Res. Lett.* **11** 034014

Andresen C G and Lougheed V L 2015 Disappearing Arctic tundra ponds: fine-scale analysis of surface hydrology in drained thaw lake basins over a 65 year period (1948–2013) *J. Geophys. Res.: Biogeosci.* **120** 466–79

Andresen C G, Tweedie C E and Lougheed V L 2018 Climate and nutrient effects on Arctic wetland plant phenology observed from phenocams *Remote Sens. Environ.* **205** 46–55

Barton K 2019 MuMIn: Multi-model inference R package version 1.43.6 (https://CRAN.R-project.org/package=MuMIn)

Bartsch A, Höfler A, Kroisleitner C and Trofaier A 2016 Land cover mapping in northern high latitude permafrost regions with satellite data: achievements and remaining challenges *Remote Sens.* **8** 979

Berner L T, Jantz P, Tape K D and Goetz S J 2018 Tundra plant above-ground biomass and shrub dominance mapped across the North Slope of Alaska *Environ. Res. Lett.* **13** 035002

Bhatt U S, Walker D A, Raynolds M, Bieniek P, Epstein H, Comiso J, Pinzon J, Tucker C and Polyakov I 2013 Recent declines in warming and vegetation greening trends over pan-Arctic Tundra *Remote Sensing* **5** 4229–54

Bhatt U S *et al* 2017 Changing seasonality of panarctic tundra vegetation in relationship to climatic variables *Environ. Res. Lett.* **12** 055003

Bhatt U S *et al* 2010 Circumpolar Arctic Tundra vegetation change is linked to Sea Ice decline *Earth Interact.* **14** 1–20

Bhatt U S *et al* 2014 Implications of Arctic Sea Ice decline for the earth system *Ann. Rev. Environ. Resour.* **39** 57–89

Bieniek P A *et al* 2015 Climate drivers linked to changing seasonality of Alaska Coastal Tundra vegetation productivity *Earth Interact.* **19** 1–29

Billings W D and Peterson K M 1980 Vegetational change and ice-wedge polygons through the Thaw-Lake Cycle in Arctic Alaska *Arctic Alpine Res.* **12** 413–32

Bronaugh D and Werner A 2019 zyp: Zhang + Yue-Pilon Trends Package. R package version 0.10-1.1 (https://CRAN.R-project.org/package=zyp)

Chapin F S 3rd *et al* 2005 Role of land-surface changes in arctic summer warming *Science* **310** 657–60

Chapman D S, Bonn A, Kunin W E and Cornell S J 2009 Random Forest characterization of upland vegetation and management burning from aerial imagery *J. Biogeogr.* **37** 37–46

Davidson S J, Santos M J, Sloan V L, Watts J D, Phoenix G K, Oechel W C and Zona D 2016a Mapping arctic Tundra vegetation communities using field spectroscopy and multispectral satellite data in North Alaska, USA *Remote Sens.* **8** 978

Davidson S J, Sloan V L, Phoenix G K, Wagner R, Fisher J P, Oechel W C and Zona D 2016b Vegetation type dominates the spatial variability in CH$_4$ emissions across multiple Arctic Tundra Landscapes *Ecosystems* **19** 1116–32

Elmendorf S C *et al* 2012 Global assessment of experimental climate warming on tundra vegetation: heterogeneity over space and time *Ecol. Lett.* **15** 164–75

Epstein H E, Raynolds M K, Walker D A, Bhatt U S, Tucker C J and Pinzon J E 2012 Dynamics of aboveground phytomass of the circumpolar Arctic tundra during the past three decades *Environ. Res. Lett.* **7** 015506

Evans J S 2019 spatialEco R package version 1.2-0 (https://github.com/jeffreyevans/spatialEco)

Fernandes R and Leblanc G S 2005 Parametric (modified least squares) and non-parametric (Theil–Sen) linear regressions for predicting biophysical parameters in the presence of measurement errors *Remote Sens. Environ.* **95** 303–16

Forbes B C, Macias-Fauria M and Zetterberg P 2010 Russian Arctic warming and 'greening' are closely tracked by tundra shrub willows *Glob. Change Biol.* **16** 1542–54

Frost G V, Epstein H E and Walker D A 2014 Regional and landscape-scale variability of Landsat-observed vegetation dynamics in northwest Siberian tundra *Environ. Res. Lett.* **9** 025004

Gandhi G M, Parthiban S, Thummalu N and Christy A 2015 Ndvi: vegetation change detection using remote sensing and Gis—a case study of vellore district *Proc. Comput. Sci.* **57** 1199–210

Goetz S J, Bunn A G, Fiske G J and Houghton R A 2005 Satellite-observed photosynthetic trends across boreal North America associated with climate and fire disturbance *Proc. Natl Acad. Sci. USA* **102** 13521–5

Hinkel K M, Eisner W R, Bockheim J G, Nelson F E, Peterson K M and Dai X 2003 Spatial extent, age, and carbon stocks in drained thaw Lake Basins on the barrow peninsula, Alaska *Arctic, Antarct., Alpine Res.* **35** 291–300

Hudson J M G and Henry G H R 2009 Increased plant biomass in a high Arctic heath community from 1981 to 2008 *Ecology* **90** 2657–63

Huemmrich K F, Kinoshita G, Gamon J A, Houston S, Kwon H and Oechel W C 2010 Tundra carbon balance under varying temperature and moisture regimes *J. Geophys. Res.* **115** G00I02

Hugelius G *et al* 2014 Estimated stocks of circumpolar permafrost carbon with quantified uncertainty ranges and identified data gaps *Biogeosciences* **11** 6573–93

IPCC 2013 *Climate Change 2013: The Physical Science Basis. Contribution of Working Group I to the Fifth Assessment Report of the Intergovernmental Panel on Climate Change* ed T F Stocker *et al* (Cambridge: Cambridge University Press) p 1535

Jia G J, Epstein H E and Walker D A 2003 Greening of arctic Alaska, 1981–2001 *Geophys. Res. Lett.* **30** 2067

Joos F, Prentice I C, Sitch S, Meyer R, Hooss G, Plattner G-K, Gerber S and Hasselmann K 2001 Global warming feedbacks on terrestrial carbon uptake under the Intergovernmental Panel on Climate Change (IPCC) Emission Scenarios *Glob. Biogeochem. Cycles* **15** 891–907

Kauth R J and Thomas G 1976 The tasselled cap–a graphic description of the spectral-temporal development of agricultural crops as seen by Landsat. LARS symposia 159 (http://docs.lib.purdue.edu/lars_symp/159)

Lara M J, Nitze I, Grosse G, Martin P and Mcguire A D 2018 Reduced arctic tundra productivity linked with landform and climate change interactions *Sci. Rep.* **8** 2345

Liljedahl A K *et al* 2016 Pan-Arctic ice-wedge degradation in warming permafrost and its influence on tundra hydrology *Nat. Geosci.* **9** 312–8

Lin D H, Johnson D R, Andresen C G and Tweedie C E 2012 High spatial resolution decade-time scale land cover change at multiple locations in the Beringian Arctic (1948–2000s) *Environ. Res. Lett.* **7** 025502

Macias-Fauria M, Karlsen S R and Forbes B C 2017 Disentangling the coupling between sea ice and tundra productivity in Svalbard *Sci. Rep.* **7** 8586

May J, Healey N, Ahrends H, Hollister R, Tweedie C, Welker J, Gould W and Oberbauer S 2017 Short-term impacts of the air temperature on greening and senescence in Alaskan Arctic Plant Tundra habitats *Remote Sens.* **9** 1338

Mishra U and Riley W J 2012 Alaskan soil carbon stocks: spatial variability and dependence on environmental factors *Biogeosciences* **9** 3637–45

Myers-Smith I *et al* 2011 Shrub expansion in tundra ecosystems: dynamics, impacts and research priorities *Environ. Res. Lett.* **6** 045509

Myers-Smith I *et al* 2019 *Complexity Revealed in the Greening of the Arctic. EcoEvoRxiv* (https://doi.org/10.32942/osf.io/mzyjk)

Natali S M *et al* 2015 Permafrost thaw and soil moisture driving CO_2 and CH_4 release from upland tundra *J. Geophys. Res.: Biogeosci.* **120** 525–37

Nitze I and Grosse G 2016 Detection of landscape dynamics in the Arctic Lena Delta with temporally dense Landsat time-series stacks *Remote Sens. Environ.* **181** 27–41

Oberbauer S F *et al* 2013 Phenological response of tundra plants to background climate variation tested using the International Tundra experiment *Phil. Trans. R. Soc.* B **368** 20120481

Oksanen J *et al* 2018 Vegan: community ecology package R package version 2.5-5 (https://CRAN.R-project.org/package=vegan)

Phoenix G K and Bjerke J W 2016 Arctic browning: extreme events and trends reversing arctic greening *Glob. Change Biol.* **22** 2960–2

Piao S *et al* 2014 Evidence for a weakening relationship between interannual temperature variability and northern vegetation activity *Nat. Commun.* **5** 5018

Ping C-L, Michaelson G J, Jorgenson M T, Kimble J M, Epstein H, Romanovsky V E and Walker D A 2008 High stocks of soil organic carbon in the North American Arctic region *Nat. Geosci.* **1** 615–9

Pinheiro J, Bates D, Debroy S, Sarkar D and Team R C 2018 nlme: Linear and nonlinear mixed effects models R package version 3.1-137 (https://CRAN.R-project.org/package=vegan)

Price D T *et al* 2013 Anticipating the consequences of climate change for Canada's boreal forest ecosystems *Environ. Rev.* **21** 322–65

R Core Team 2018 R: A Language and Environment for Statistical Computing R Foundation for Statistical Computing (https://www.R-project.org/)

Raynolds M K and Walker D A 2016 Increased wetness confounds Landsat-derived NDVI trends in the central Alaska North Slope region, 1985–2011 *Environ. Res. Lett.* **11** 085004

Raynolds M K, Walker D A, Epstein H E, Pinzon J E and Tucker C J 2011 A new estimate of tundra-biome phytomass from trans-Arctic field data and AVHRR NDVI *Remote Sens. Lett.* **3** 403–11

Romanovsky V, Smith S L, Shiklomanov N, Streletskiy D A, Isaken K, Kholodov A L, Christensen H H, Drozdov D S, Malkova G V and Marchenko S 2017 [The Arctic] Terrestrial permafrost [in 'State of the Climate in 2016'] *Bull. Am. Meteorol. Soc.* **98** S147–51

Schuur E A *et al* 2013 Expert assessment of vulnerability of permafrost carbon to climate change *Clim. Change* **119** 359–74

Schuur E A *et al* 2015 Climate change and the permafrost carbon feedback *Nature* **520** 171–9

Sen P K 1968 Estimates of the regression coefficient based on Kendall's Tau *J. Am. Stat. Assoc.* **63** 1379–89

Serreze M C and Francis J A 2006 The Arctic amplification debate *Clim. Change* **76** 241–64

Spencer R G M, Mann P J, Dittmar T, Eglinton T I, Mcintyre C, Holmes R M, Zimov N and Stubbins A 2015 Detecting the signature of permafrost thaw in Arctic rivers *Geophys. Res. Lett.* **42** 2830–5

Stow D A *et al* 2004 Remote sensing of vegetation and land-cover change in Arctic Tundra ecosystems *Remote Sens. Environ.* **89** 281–308

Sturtevant C S and Oechel W C 2013 Spatial variation in landscape-level CO_2 and CH_4 fluxes from arctic coastal tundra: influence from vegetation, wetness, and the thaw lake cycle *Glob. Change Biol.* **19** 2853–66

Suzuki R, Nomaki T and Yasunari T 2001 Spatial distribution and its seasonality of satellite-derived vegetation index (NDVI) and climate in Siberia *Int. J. Climatol.* **21** 1321–35

Tape K E N, Sturm M and Racine C 2006 The evidence for shrub expansion in Northern Alaska and the pan-Arctic *Glob. Change Biol.* **12** 686–702

Theil H 1992 A rank-invariant method of linear and polynomial regression analysis *Henri Theil's Contributions to Economics and Econometrics: Econometric Theory and Methodology* ed B Raj and J Koerts (Dordrecht: Springer Netherlands) (https://doi.org/10.1007/978-94-011-2546-8)

Treat C C *et al* 2018 Tundra landscape heterogeneity, not interannual variability, controls the decadal regional carbon balance in the Western Russian Arctic *Glob. Change Biol.* **24** 5188–204

Van Beijma S, Comber A and Lamb A 2014 Random forest classification of salt Marsh vegetation habitats using quad-polarimetric airborne SAR, elevation and optical RS data *Remote Sens. Environ.* **149** 118–29

Villarreal S, Hollister R D, Johnson D R, Lara M J, Webber P J and Tweedie C E 2012 Tundra vegetation change near Barrow, Alaska (1972–2010) *Environ. Res. Lett.* **7** 015508

Walker D A *et al* 2005 The Circumpolar Arctic vegetation map *J. Vegetation Sci.* **16** 267–82

Webber P J 1978 Spatial and temporal variation of the vegetation and its production, Barrow, Alaska *Vegetation and Production Ecology of an Alaskan Arctic Tundra* ed L L Tieszen (New York, NY: Springer New York) (https://doi.org/10.1007/978-1-4612-6307-4)

Westergaard-Nielsen A, Lund M, Pedersen S H, Schmidt N M, Klosterman S, Abermann J and Hansen B U 2017 Transitions in high-Arctic vegetation growth patterns and ecosystem productivity tracked with automated cameras from 2000 to 2013 *Ambio* **46** 39–52

Wilson C J, Gangodagamage C and Rowland J 2013 *Digital Elevation Model, 0.5 m, Barrow Environmental Observatory, Alaska,*

2012. Next Generation Ecosystem Experiments Arctic Data Collection Dataset (Oak Ridge, TN: Oak Ridge National Laboratory) (https://doi.org/10.5440/1109234)

Yarbrough L D, Easson G and Kuszmaul J S 2005 QuickBird 2 tasseled cap transform coefficients: a comparison of derivation methods *Conf. Proc. Pecora 16 'Global Priorities in Land Remote Sensing' (23–27 October 2005 Sioux Falls, South Dakota)* pp 23–7

Yue S, Pilon P, Phinney B and Cavadias G 2002 The influence of autocorrelation on the ability to detect trend in hydrological series *Hydrol. Processes* **16** 1807–29

Zeng H, Jia G and Epstein H 2011 Recent changes in phenology over the northern high latitudes detected from multi-satellite data *Environ. Res. Lett.* **6** 045508

Zhang X, He J, Zhang J, Polyakov I, Gerdes R, Inoue J and Wu P 2012 Enhanced poleward moisture transport and amplified northern high-latitude wetting trend *Nat. Clim. Change* **3** 47–51

Zhang X, Jayavelu S, Liu L, Friedl M A, Henebry G M, Liu Y, Schaaf C B, Richardson A D and Gray J 2018 Evaluation of land surface phenology from VIIRS data using time series of PhenoCam imagery *Agric. Forest Meteorol.* **256–257** 137–49